Contribution from the Departments of Chemistry, University of Notre Dame, Notre Dame, Indiana 46556, and University of Missouri—Rolla, Rolla, Missouri 65401

Main-Group Chemistry on a Metal Framework: Preparation and Characterization of $B_2H_6Fe_2(CO)_6$ and Its Conjugate Base $[B_2H_5Fe_2(CO)_6]^-$

G. B. Jacobsen,† E. L. Andersen,† C. E. Housecroft,† F.-E. Hong,† Margaret L. Buhl,‡ Gary J. Long,‡ and T. P. Fehlner*†

Received May 27, 1987

The preparation and spectroscopic characterization of $B_2H_6Fe_2(CO)_6$ and the anion $[B_2H_5Fe_2(CO)_6]^-$ are described. The proposed structures of both compounds contain diboron-bridged diiron hexacarbonyl cores. The static structure of the former has two terminal, one B–B bridging, and three Fe–B bridging hydrogens while the latter has two terminal, one B–B bridging, and two Fe–B bridging hydrogens. Both compounds exhibit fluxional processes involving terminal and bridging hydrogens via mechanisms involving correlated hydrogen movements of a type that depends on the number of bridging hydrogens. The neutral and anionic compounds react with $Fe_2(CO)_9$ to produce $HFe_4(CO)_{12}BH_2$ and $[HFe_4(CO)_{12}BH]^-$ plus $[Fe_3(CO)_{10}BH_2]^-$, respectively. These reactions are viewed as cluster expansion by the addition of $Fe(CO)_3$ fragments and formal replacement of a BH fragment by a $Fe(CO)_3$ fragment. Fenske–Hall calculations are used to explore some of the consequences of different hydrogen atom arrangements on a two-boron–two-iron framework.

The so-called "borane analogy"[1] is valuable because the concept emphasizes similarities between boranes and metal clusters—compounds containing atoms of apparently disparate properties. Not unexpectedly, more recent accounts of the "borane analogy" have emphasized the differences, i.e., that boranes and metal clusters with analogous cluster core structures are expected to have distinctly different spectroscopic and chemical properties.[2] The existence of hybrids of boranes and metal clusters, metallaboranes,[3] presents an interesting experimental challenge. When will these hybrids exhibit the properties of metal clusters or those of boranes? Indeed, will these hybrids show new properties not seen in either of the prototypes? Earlier we have discussed ferraboranes containing more boron than iron atoms[4] and, more recently, compounds containing a single boron atom and three or four iron atoms.[5] In the latter system, $HFe_4(CO)_{12}BH_2$, the main-group fragment is so perturbed by being bound to four metal atoms that complete deprotonation of the cluster to yield $[Fe_4(CO)_{12}B]^{3-}$ is possible;[6] i.e., the boron hydride has completely lost its hydridic character. Herein we present the characterization of a two-boron–two-iron metallaborane, $B_2H_6Fe_2(CO)_6$ (I), which, stoichiometrically, lies midway between the borane B_4H_8, known as a transient species,[7] and the unstable $H_4Fe_4(CO)_{12}$ cluster, for which the ruthenium and osmium analogues are known.[8] Alternatively, I can be formally considered as a diborane moiety coordinated to a diiron hexacarbonyl fragment.

The isolation of the neutral compound $B_2H_6Fe_2(CO)_6$ has been reported earlier;[9] however, as is detailed below, the static distribution of endo-hydrogen atoms (Ib, Chart I) postulated on the basis of 100-MHz ^1H NMR data at 25 °C is incorrect. The correct structure (Ia, Chart I) and the previously postulated one (Ib) differ in the most stable position of one hydrogen atom. Indeed, the hydrogen arrangement Ib proposed previously defines a possible intermediate in the fluxional processes described below. We demonstrate that the mechanism of this fluxional process requires the correlation of hydrogen atom movement. Comparison with the fluxional behavior of the conjugate base produced by deprotonation yields a relationship among FeHB, BHB, and BH hydrogens that is not present in the analogous $HFe_3(CO)_9BH_4$ cluster.[5] Finally, our observations on these compounds serve to further define the factors important in determining the stable hydrogen location and mobility on main-group–transition-metal clusters.[10]

Results

Static Structure of the Neutral Compound. Although we have been unsuccessful in obtaining crystals of either the neutral or anionic ferraborane, the basic cluster core of the compound is almost certainly a distorted B_2Fe_2 tetrahedron with three carbonyl ligands on each iron atom (Chart I). However, as intimated above, the distribution of hydrogen atoms on this basic core is not as

Chart I

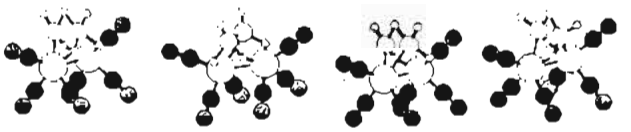

Ia Ib II(cis) II(trans)

Table I. ^1H NMR Spectral Data for $B_2H_6Fe_2(CO)_6$ and $[B_2H_5Fe_2(CO)_6]^-$[a]

δ[b]	fwhm,[c] Hz	fwhm,[d] Hz	rel intens	assignt	J_{BH}, Hz[e]
		$B_2H_6Fe_2(CO)_6$[f]			
2.31		220	2	BH(term)	
−2.44		64	1	BHB	
−12.88		80	1	BHFe	
−15.57		100	2	BHFe	
		$[B_2H_5Fe_2(CO)_6]^-$[g]			
2.2		230	2	BH(term)	
−2.6	115	65	1	BHB	
−14.2	350	90	2	FeHB	45
7.58–7.56[h]			20	Ph_4As^+	

[a] Obtained at 300 MHz in CD_2Cl_2. [b] Negative chemical shifts are upfield of TMS = 0 ppm. [c] Width at half-height at 20 °C. [d] Width at half-height at lowest temperature (thermally decoupled). [e] Coupling constant measured at −20 °C. [f] Low-temperature spectrum at −90 °C. [g] Low-temperature spectrum at −60 °C: Ph_4As^+ salt. [h] Parameters for the $N(C_2H_5)_3H^+$ salt were identical. Cation resonances observed at 20 °C: δ 1.40 (CH_3), 3.10 (NH), 3.45 (CH_2). The resonance at δ 3.1 is broad and shifts to lower field at lower temperatures.

† University of Notre Dame.
‡ University of Missouri—Rolla.

(1) Wade, K. *Adv. Inorg. Chem. Radiochem.* **1976**, *18*, 1. Mingos, D. M. P. *Nature (London), Phys. Sci.* **1972**, *236*, 99.
(2) Wooley, R. G. *Inorg. Chem.* **1985**, *24*, 3525.
(3) Grimes, R. N., Ed. *Metal Interactions with Boron Clusters*; Plenum: New York, 1982. Housecroft, C. E.; Fehlner, T. P. *Adv. Organomet. Chem.* **1982**, *21*, 57. Kennedy, J. D. *Prog. Inorg. Chem.* **1984**, *32*, 519; **1984**, *34*, 211.
(4) Fehlner, T. P. *J. Am. Chem. Soc.* **1980**, *102*, 3424. Haller, K. J.; Andersen, E. L.; Fehlner, T. P. *Inorg. Chem.* **1981**, *20*, 309. Housecroft, C. E. *Inorg. Chem.* **1986**, *25*, 3108.
(5) Vites, J.; Housecroft, C. E.; Eigenbrot, C.; Buhl, M. L.; Long, G. J.; Fehlner, T. P. *J. Am. Chem. Soc.* **1986**, *108*, 3304. Housecroft, C. E.; Fehlner, T. P. *J. Am. Chem. Soc.* **1986**, *108*, 4867. Fehlner, T. P.; Housecroft, C. E.; Scheidt, W. R.; Wong, K. S. *Organometallics* **1983**, *2*, 825. Housecroft, C. E.; Buhl, M. L.; Long, G. J.; Fehlner, T. P. *J. Am. Chem. Soc.* **1987**, *109*, 3323.
(6) Rath, N. P.; Fehlner, T. P. *J. Am. Chem. Soc.* **1987**, *109*, 5273.
(7) Hollins, R. E.; Stafford, F. E. *Inorg. Chem.* **1973**, *12*, 798.
(8) Chini, P.; Heaton, B. T. *Top. Curr. Chem.* **1977**, *71*, 1.
(9) Andersen, E. L.; Fehlner, T. P. *J. Am. Chem. Soc.* **1978**, *100*, 4606.

0020-1669/87/1326-4040$01.50/0

Table II. ^{11}B NMR Spectral Parameters for $B_2H_6Fe_2(CO)_6$ and $[B_2H_5Fe_2(CO)_6]^-$

δ^a	T, °C	multiplicity	J_{BH}, Hz
	$B_2H_6Fe_2(CO)_6$[b]		
−24.2	20	dt	65, 60[c]
	$[B_2H_5Fe_2(CO)_6]^-$[d]		
−17.4	20	td	105, 25
−17.4	−20	ddd	125[e]

[a] Chemical shifts are quoted as negative upfield of $BF_3{\cdot}OEt_2$ = 0 ppm. [b] Obtained at 96.3 MHz in hexanes. [c] Coupling constants measured from double irradiation experiments. [d] Obtained at 96.3 MHz in CD_2Cl_2. [e] Only terminal BH coupling resolved due to line broadening at lower temperatures.

Table III. Mössbauer Spectral Parameters for $B_2H_6Fe_2(CO)_6$ and $[B_2H_5Fe_2(CO)_6]^-$[a]

assignt	δ, mm/s	ΔE_Q, mm/s	Γ	% area	Z_{eff}
		$B_2H_6Fe_2(CO)_6$			
Fe(HHFe)[b]	−0.02	1.24	0.24	42.25[c]	3.2877
Fe(HBFe)	0.05	1.08	0.48	42.25[c]	3.2458
impurity	1.34	2.62	0.42	15.50	
		$[B_2H_5Fe_2(CO)_6]$PPN			
Fe(HHFe)	−0.01	1.27	0.28	38.54[c]	3.2706
Fe(HBFe)	0.05	1.44	0.23	22.93	3.2303
Fe(BBFe)	0.10	0.22	0.42	38.54[c]	3.2022

[a] All data obtained at 78 K and given relative to natural-abundance room-temperature α-iron foil. [b] Atoms in parentheses are the nearest neighbors to iron other than CO. [c] Values constrained in a ratio of 1 to 1.

obvious. A combination of variable-temperature NMR, Mössbauer spectroscopy and infrared spectroscopy was required to fully resolve the hydrogen distribution.

The chemical shifts of the observed resonances in the ^1H NMR spectrum of I at −90 °C (Table I) show the presence of two BH terminal protons, one BHB bridge proton, and three BHFe protons (in two distinct environments). This eliminates structure Ib. Assuming only edge-bridging or terminal protons,[11] only structure Ia is possible. As shown in Chart I, Ia has three types of edge FeHB protons, which is consistent with the ^1H NMR data if an FeHB proton exchanges with the adjacent FeB edge rapidly on the NMR time scale at −90 °C. There are two possibilities, one yielding equivalent iron atoms and inequivalent borons and the other inequivalent iron atoms and equivalent borons. The fact that a single (if broad) $^{11}B\{^1H\}$ NMR resonance (Table II) is observed at −90 °C (invariant chemical shift from −90 to +25 °C) requires the latter process, in which the proton moves across a B_2Fe face of the tetrahedral cluster. Note that in a completely static Ia structure both the irons and borons are in different environments.

Further information on the chemical environment of the iron atoms is given by the low-temperature Mössbauer spectrum of I, which is shown in Figure 1a, with the parameters being given in Table III. The Mössbauer spectrum of I shows two inequivalent iron sites and about 16% of a high-spin Fe(II) impurity. This impurity has no effect upon the assignment of the doublets in the spectrum to specific iron sites. As this is a solid-state spectrum, the presence of two types of iron atoms is consistent with structure Ia. The assignment of the quadrupole doublets proceeds from a consideration of the electron-withdrawing power or electro-

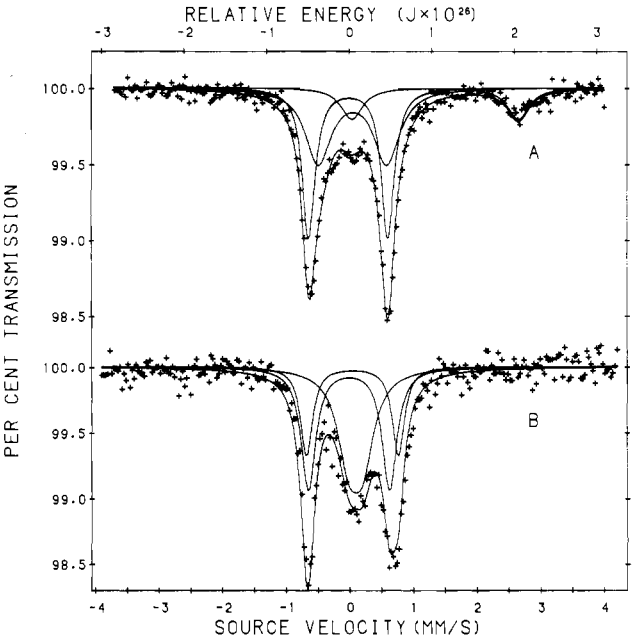

Figure 1. Mössbauer spectra of (A) $B_2H_6Fe_2(CO)_6$ and (B) $[B_2H_5Fe_2(CO)_6]$PPN at 78 K.

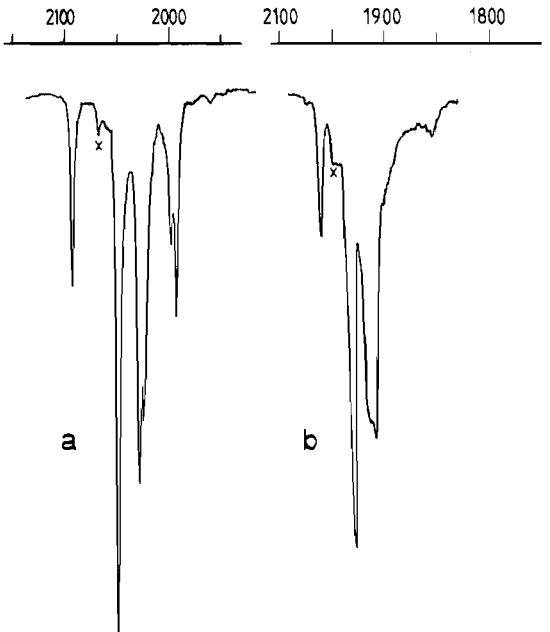

Figure 2. Infrared spectra of (a) $B_2H_6Fe_2(CO)_6$ and (b) $[B_2H_5Fe_2(CO)_6]As(C_6H_5)_3$ in the carbonyl region. Note that the scales are different and that the ×'s denote the most intense bands of $B_3H_7Fe_2(CO)_6$ and $[B_3H_6Fe_2(CO)_6]^-$, respectively. These related ferraboranes are formed in the preparative procedures and are difficult to remove.

negativity of the B and H atoms in the B_2H_6 moiety. Because the B atom in the B_2H_6 moiety is a stronger Lewis acid than is the hydride ion, it has a greater electron-withdrawing power. This causes the s-electron density about the Fe(HBFe) site to be lower than that about the Fe(HHFe) site. For iron-57 Mössbauer spectra, the s-electron density about the iron site and the isomer shift have an inverse relationship; i.e., as the electron density increases, the isomer shift decreases. This inverse relationship leads to the assignment of the inner doublet (highest isomer shift, lowest s-electron density) to the Fe(HBFe) site and the outer doublet (lowest isomer shift, highest s-electron density) to the Fe(HHFe) site.

The same assignments are obtained when one considers the effective nuclear charge, Z_{eff}, experienced by the iron 4s electrons, as calculated by the method of Slater using the iron valence-orbital

(10) Lynam, M. M.; Chipman, D. M.; Barreto, R. D.; Fehlner, T. P. *Organometallics* **1987**, *6*, 2405.

(11) Static face-bridging structures cannot be ruled out entirely; however, the disposition of the hydrogens would be far from tetrahedral and H–H distances would be small. For example, a structure with one Fe_2–μ_3H–B and two Fe–μH–B protons, having equivalent irons but different borons, is consistent with the low-temperature ^1H spectra but not the ^{11}B NMR spectra. Likewise, a structure with one Fe–μ_3H–B_2 and two Fe–μH–B protons also accounts for the ^1H spectra, but the fluxional behavior exhibited by I rules it out.

Table IV. Infrared Spectral Data for $B_2H_6Fe_2(CO)_6$ and $[B_2H_5Fe_2(CO)_6]^-$

ν, cm^{-1}	intens	assignt[a]	ν, cm^{-1}	intens	assignt[a]
		$B_2H_6Fe_2(CO)_6$[b]			
2530	w	B–H str	2026	s	CO ν_2 or ν_6
2090	s	CO ν_1	2022	s	
2046	vs	CO ν_4	1996	s	CO ν_6 or ν_2
			1990	s	
		$[B_2H_5Fe_2(CO)_6]^-$[c]			
2470	w	B–H str	1935	sh	CO ν_2 or ν_6
2022	m	CO ν_1	1928	m	CO ν_6 or ν_2
1965	s	CO ν_4			

[a] Nomenclature of ref 13 with idealized C_{2v} symmetry. [b] In hexane. [c] Ph_4As^+ salt in toluene.

occupancies obtained from Fenske–Hall calculations.[12] The use of the orbital occupancies alone to make the assignments, does not, of course, take into account deshielding effects from π bonding. The expected result of decreasing isomer shift with increasing effective nuclear charge is indeed obtained. The calculated values of Z_{eff} are given in Table III. Independently of whether the specific assignments are correct, the spectrum shows the presence of inequivalent iron atoms, which is consistent with structure Ia but not with Ib.

The infrared spectrum of I in the carbonyl region is shown in Figure 2a, and the data are compiled in Table IV. Infrared spectra of many compounds containing a $M_2(CO)_6$ fragment have been reported, and the spectra of those containing a bridged $M_2(CO)_6$ fragment with C_{2v} symmetry are particularly well understood.[13] Five CO stretches are allowed by symmetry, but generally one is very weak and often hidden. Further, two absorptions are frequently accidentally degenerate. Hence, such compounds commonly exhibit only three or four bands. Even when substituents introduce asymmetry in the bridging ligand but without changing the connectivity to iron, the observed spectrum is often that expected for C_{2v} symmetry. Not surprisingly then, I exhibits a spectrum qualitatively consistent with that of a molecule containing a C_{2v} bridged $M_2(CO)_6$ fragment. Note, however, that there are two significant differences. First, the splitting (31 cm^{-1}) between the ν_2 and ν_6 bands is large for a molecule of C_{2v} symmetry. Second, each of these bands in turn consists of two components split by 5–6 cm^{-1}. These differences suggest that the two iron atoms are significantly different. Assuming that I in solution exists in a single isomeric form, this difference requires the placement of the B_2H_6 fragment such that the molecular symmetry is less than C_{2v} and that the nearest-neighbor atoms for the two iron sites are different. These results are consistent with structure Ia (C_1 symmetry) but not Ib (C_{2v} symmetry). A single BH(terminal) stretch is observed at 2442 cm^{-1}; however, the band is broad and does not eliminate structure Ia. Note that this static structure is chiral.

Static Structure of the Anion. $[B_2H_5Fe_2(CO)_6]^-$ (II) results quantitatively from the deprotonation of I by a variety of bases. Its infrared spectrum (Figure 2b, Table IV) again exhibits the four bands in the CO stretching region expected for a compound containing a bridged $M_2(CO)_6$ fragment. The mean value of the four CO absorptions of II is shifted 76 cm^{-1} to lower energy relative to that of I. This is consistent with the anionic nature of II. After taking into account the general shift to lower energy, we find that the two frequencies most affected by deprotonation are ν_2 and ν_6. These are associated with the four equatorial CO's and suggest that the proton is removed from an FeHB position. Compared to the frequencies of the neutral compound, ν_2 and ν_6 are closer in energy; i.e., the spectrum is very similar to that observed for molecules like $S_2Fe_2(CO)_6$.[14] This suggests a structure similar to that of the neutral compound I but with iron "ligand" environments more closely approaching C_{2v} symmetry. This is easily achieved by removing a BHFe proton from an iron–boron edge in Ia, thereby producing structure II(trans), with equivalent iron atoms, or II(cis), with inequivalent iron atoms. Although there is no infrared evidence for more than one species in solution, the broader lines due to the anionic nature of II may hide additional species. Again, a single BH(terminal) absorption is observed. However, it is 21 cm^{-1} higher in energy than in the neutral compound. This is consistent with the higher terminal BH coupling constant in the anion (see below), thereby suggesting an increase in the BH(terminal) bond strength on deprotonation. In previous work[5] we have noted that sequential loss of BHFe hydrogens connected to a BH fragment increases the B 2s character of the BH terminal interaction. A similar effect appears to be operative here.

The Mössbauer spectrum of II is shown in Figure 1B, and the parameters are given in Table III. Unexpectedly, the spectrum consists of three quadrupole doublets of similar intensity. Ruling out impurities (see Experimental Section), this can only be explained by postulating the existence of isomers in the solid state at 78 K. As the solution infrared spectrum at 25 °C does not permit species with grossly different structures, this isomerism is attributed to different hydrogen positions; i.e., structures II(cis) and II(trans) are isomers that have "cis" and "trans" arrangements of the FeHB bridging protons. The former has inequivalent irons whereas the latter has equivalent irons. Hence, to explain the Mössbauer spectrum, we postulate an approximate 1:3 "trans" to "cis" ratio in the solid state. To make the appropriate assignments, the relative s-electron-withdrawing power of the B and H in the B_2H_6 moiety is again considered. The Fe sites, in order to increasing s-electron density, are then Fe(BBFe) < Fe(HBFe) < Fe(HHFe). Considering the negative relationship between the s-electron density and the isomer shift, the Fe sites in order of increasing isomer shift are Fe(HHFe) < Fe(HBFe) < Fe(BBFe). The outer doublet, therefore, has been assigned to the equivalent Fe(HBFe) sites of the trans isomer. The remaining two doublets are then assigned to the cis isomer. These remaining doublets have been fit with their areas constrained in a ratio of 1:1. The middle doublet is assigned to the Fe(HHFe) site, while the inner doublet is assigned to the Fe(BBFe) site. Similar iron sites are expected to have similar isomer shifts, and this is indeed the case (see Table III). Also, the Fe(BHFe) site of the trans compound has as expected an isomer shift equal to the average isomer shift of the Fe(HHFe) and the Fe(BBFe) sites. The assignments are also consistent with the effective nuclear charge experienced by the iron 4s electrons.

The low-temperature ^1H NMR spectrum (Table I) and selective $^{11}B\{^1H\}$ spectra (Table II) demonstrate the presence of two BH terminal, one BHB bridge, and two FeHB bridge protons in the static structure of II. Either of the two structures II(cis) and II(trans) can accommodate the NMR data; i.e., the FeHB resonance is broad so that a small difference between the chemical shifts of the FeHB protons in structures II(cis) and II(trans) may not be observed, particularly as the two species are not equally abundant.

Fluxional Behavior. As is well-known, the incorporation of a main-group hydride fragment into a metal-cluster bonding network can lead to rates of exchange between main-group hydrogens and metal hydrogens comparable to the frequency corresponding to the chemical shift difference of the types of hydrogens.[15] This is the case with both I and II. After an increase in the temperature from −90 to +20 °C, the ^1H NMR spectrum of II exhibits an unchanged BHB resonance and the partial collapse of the BH terminal and FeHB resonances. Further increase in temperature results in the loss of the latter two signals, but coalescence was not observed up to 50 °C. These observations require a fluxional process making the BH terminal and FeHB proton pairs in structures II(cis) and II(trans) equivalent without participation

(12) Benson, C. G.; Long, G. J.; Bradley, J. S.; Kolis, J. W.; Shriver, D. F. *J. Am. Chem. Soc.* **1986**, *108*, 1898.
(13) Bor, G. *J. Organomet. Chem.* **1975**, *94*, 181.
(14) Maresca, L.; Greggio, F.; Sbrignadello, G.; Bor, G. *Inorg. Chim. Acta* **1971**, *5*, 667.
(15) Johnson, B. F. G., Ed. *Transition Metal Clusters*; Wiley: New York, 1980.

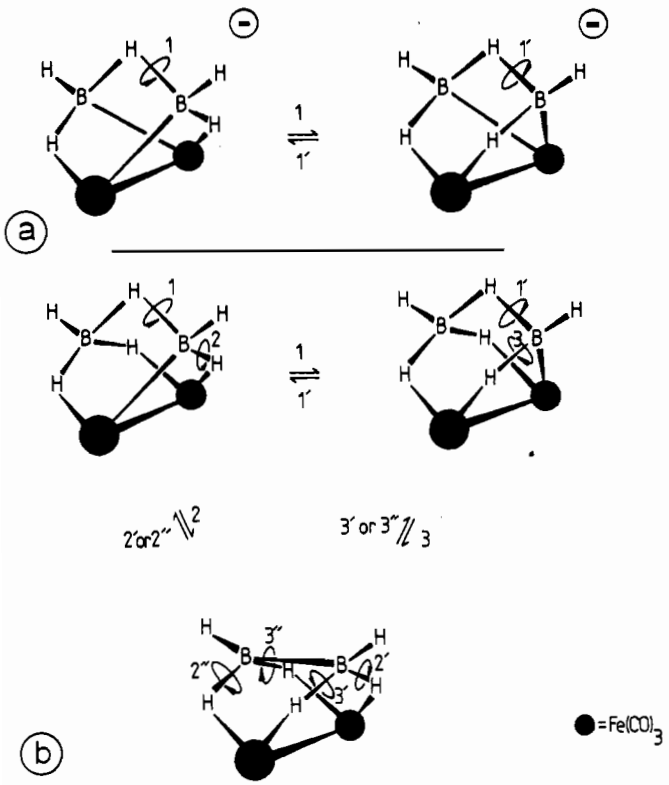

Figure 3. Proposed formal mechanisms for the hydrogen fluxionality in (a) $[B_2H_5Fe_2(CO)_6]^-$ and (b) $B_2H_6Fe_2(CO)_6$.

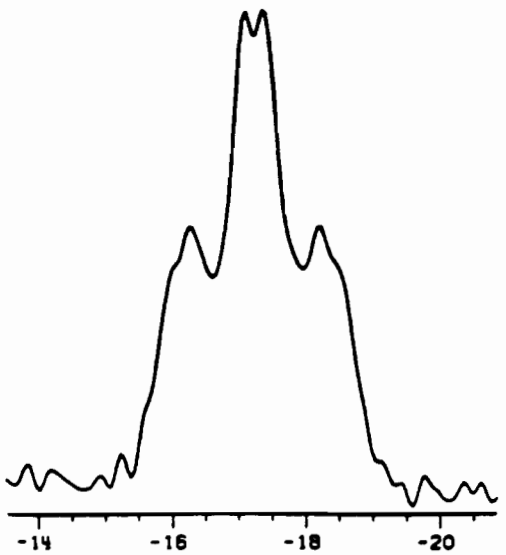

Figure 4. Line-narrowed proton-coupled ^{11}B NMR spectrum of $[B_2H_5Fe_2(CO)_6]As(C_6H_5)_4$ in CH_2Cl_2 at 20 °C.

of the BHB proton. A possible mechanism for this process is shown in Figure 3a, whereby the BH_2 fragment of an sp^3 B is rotated about the BH(bridge) axis. In agreement with this interpretation, the ^{11}B NMR spectrum at 20 °C exhibits a doublet of triplets (Figure 4 and Table II). The small coupling (25 Hz) is attributed to the BHB proton, while the larger coupling (105 Hz) is presumed to be the average of a BH(terminal) proton and a FeHB proton.[16] As expected then, at lower temperatures a broad, apparent doublet is observed with a coupling of 125 Hz (Table II). Because of increasing line widths at the lower temperatures, the smaller bridge couplings could not be observed.

The variable-temperature ^1H NMR spectra of I are shown in Figure 5. As the temperature increases from −90 °C, all reso-

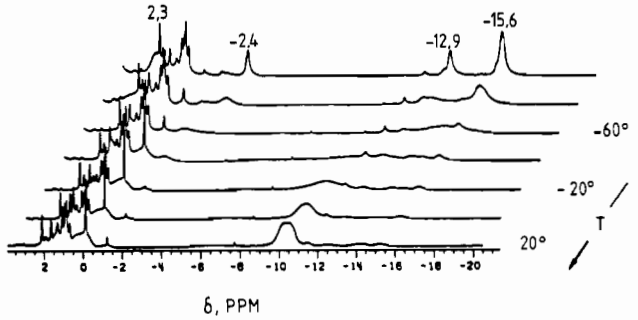

Figure 5. ^1H NMR spectra of $B_2H_6Fe_2(CO)_6$ as a function of temperature in CD_2Cl_2. The bottom spectrum was acquired at 20 °C, and the temperatures for the succeeding spectra decrease in nominal 20 °C steps. The sharp resonances in the methyl region are impurities.

Scheme I

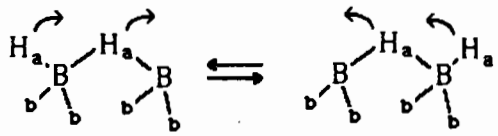

nances collapse. Subsequently, a resonance appears at 0.2 ppm (2 H) followed by one at −10.3 ppm (4 H). This constitutes the 100-MHz room-temperature spectrum previously reported for this compound.[9] The only possible rationalization of this observation is that as the temperature increases, one terminal proton and the BHB bridge proton become equivalent (calculated chemical shift −0.1 ppm) while at the same time the other four protons (one BH terminal and three FeHB protons) become equivalent (calculated chemical shift −10.2 ppm). The mechanism by which these two sets of protons attain different average environments must be an intramolecular process because BH coupling is observed at the high-temperature limit (see below). The fact that only one BH terminal proton and the BHB proton coalesce eliminates a structure with equivalent borons and is consistent with structure Ia.

The proposed mechanism for this process is shown in Figure 3b. This mechanism assumes that the protons around the boron coordinated to four hydrogens (see Ia) are frozen whereas those around the second boron are free to move by virtue of the existence of an adjacent vacant BFe edge. Formal rotation of the BH_2 fragment of the tetrahedral boron around the BH(bridge) axis (steps 1 and 1′ in Figure 3b) exchanges BHFe and BH(terminal) on the boron coordinated to three hydrogens. This is the same process postulated for the anion above. If, in addition, we postulate rapid formal rotation around the BHFe bond axis (steps 2 and 3 in Figure 3b), then we achieve the symmetrical C_{2v} structure (Ib) originally proposed as the static structure for I. Rotations 2′ and 3′ return us to structure Ia. No C_{2v} intermediate need be invoked if rotation 2′ is synchronous with rotation 3 (and rotation 2 is synchronous with rotation 3′). Independently of whether a synchronous or asynchronous mechanism operates, the net result is to make one BH(terminal) and three FeHB protons equivalent and one BH(terminal) proton and one BHB proton equivalent, as required by the experimental observations. In effect, as is illustrated by Scheme I, two protons are moving back and forth like "windshield wipers", permitting alternate scrambling of the other two pairs of protons on the two borons. Note that the mechanism proposed is a variation of that suggested for the selective scrambling of the bridging protons in B_6H_{10} and $[B_5H_8]^-$.[17] One might envision the BH_n units as a set of cog wheels that can only rotate when there is a vacancy to accept a BH "cog".

The selective $^{11}B\{^1H\}$ NMR (Table II) are consistent with the proposed mechanism. Decoupling the δ −10.3 protons leads to a doublet with a BH coupling of 65 Hz, which, according to the mechanism, should be the average of BH(terminal) and BH-

(16) Shore, S. G. In *Boron Hydride Chemistry*; Muetterties, E. L., Ed.; Academic: New York, 1975; p 79.

(17) Shore, S. G.; Johnson, H. D., II. *Chem. Commun.* **1972**, 1128. Johnson, H. D., II; Geanangel, R. A.; Shore, S. G. *Inorg. Chem.* **1970**, *9*, 1970.

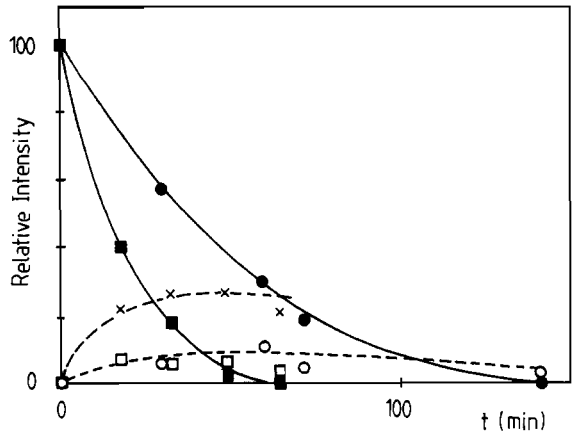

Figure 6. Reaction of $[B_2H_5Fe_2(CO)_6]^-$ and $B_2H_6Fe_2(CO)_6$ with $Fe_2(CO)_9$ as followed by ^{11}B NMR spectroscopy: (●) loss of I; (■) loss of II; (□ and ○) formation of III and IV, respectively; (×) formation of $[BH_2Fe_3(CO)_{10}]^-$.

(bridge) coupling constants. If one estimates[18] the former from the BH stretching frequency in the infrared spectrum as 110 Hz, the latter is 20 Hz, which is very reasonable. Note that the multiplicity of the signal is 2 rather than 3, indicating that the two H_a protons (Scheme I) never completely exchange, which is consistent with the proposed mechanism. Decoupling the δ 0.2 signal results in a triplet in the boron spectrum with a BH coupling of 60 Hz, which should be the average coupling constant of one BH(terminal) and three FeHB protons. Again taking the coupling constant of the former as 110 Hz, 43 Hz is calculated for the latter, which, on the basis of measured coupling constants for the FeHB proton in closely related compounds,[4,5] is a reasonable value.

The fluxional behaviors of I and its conjugate anion II present an interesting contrast. Mechanisms 1 and 1′ (Figure 3) occur in both, while mechanisms 2 and 2′ and mechanisms 3 and 3′ are not observed in II. If the C_{2v} structure (Ib) were a real intermediate in the fluxional processes of I, mechanisms 2 and 2′ and mechanisms 3 and 3′ would also be expected in II. As for most monoboron ferraboranes and boron hydrides, deprotonation leads to more facile fluxional behavior.[4,5,16] Thus, the 3,2′- or 2,3′- "rotations" probably occur synchronously in I so as to preserve the BHB interaction. This suggests that the BHB interaction is energetically preferred over the FeHB interaction and, hence, is retained in the fluxional processes.

Reactivity. Previously we have suggested that the nonbridged edge of I should constitute a site of Lewis basicity, as BB bonds in polyhedral boranes have basic character.[16] Further, we have demonstrated the clean formation of $[HFe_4(CO)_{12}BH]^-$ (IV) from the reaction of $[HFe_3(CO)_9BH_3]^-$ and $Fe_2(CO)_9$.[5,19] Hence, we considered both I and II as reasonable precursors to the presently unknown ferraboranes $B_2H_6Fe_3(CO)_9$ and $[B_2H_5Fe_3(CO)_9]^-$.

The reaction of I with $Fe_2(CO)_9$, a formal source of $Fe(CO)_3$ fragments, leads to the formation of $HFe_4(CO)_{12}BH_2$ (III).[9] Figure 6 shows the production of III as a function of time and demonstrates that the maximum yield of the "butterfly" cluster is only 10%. No other boron-containing products are seen by ^{11}B NMR spectroscopy. The reaction of II with $Fe_2(CO)_9$ is more rapid, but the analogous cluster product, $[HFe_4(CO)_{12}BH]^-$ (IV), is observed in approximately the same yield as that of III from the reaction of I with $Fe_2(CO)_9$. However, an additional species, $[Fe_3(CO)_{10}BH_2]^-$, is observed in the anionic reaction and constitutes the predominant product (Figure 6). The similarity in the yields of III and IV suggests a similarity in reaction mechanisms even though $[Fe_3(CO)_{10}BH_2]^-$ is observed in the reaction involving II but the analogous compound, $HFe_3(CO)_{10}BH_2$, is not observed in the case of I. To investigate the latter point, we have examined the direct reaction of $HFe_3(CO)_{10}BH_2$ and $[Fe_3(CO)_{10}BH_2]^-$ with $Fe_2(CO)_9$. Under the same reaction conditions, no reaction of $[Fe_3(CO)_{10}BH_2]^-$ with $Fe_2(CO)_9$ is observed in 4 h, and therefore, when produced in the reaction of II with $Fe_2(CO)_9$, $[Fe_3(CO)_{10}BH_2]^-$ will remain as an observable product. On the other hand, $HFe_3(CO)_{10}BH_2$ disappears (80% in 100 min) in the presence of $Fe_2(CO)_9$ without the production of a ^{11}B NMR observable product. Therefore, if $HFe_3(CO)_{10}BH_2$ is produced in the reaction of I with $Fe_2(CO)_9$, it would be present only as an intermediate at low levels. Therefore, we postulate similar reaction pathways for neutral and anionic compounds. Compounds III and IV are observed, as they react rather sluggishly with $Fe_2(CO)_9$, while $[Fe_3(CO)_{10}BH_2]^-$ is observed and $HFe_3(CO)_{10}BH_2$ is not because of differing reactivities with $Fe_2(CO)_9$. The ability to detect and isolate a given ferraborane depends on its stability under the reaction conditions.

Reactions of metal clusters with sources of metal fragments resulting in either cluster expansion or metal-fragment substitution are known.[15,20] If one postulates that the reaction of a metallaborane with a source of metal fragments can result in cluster expansion or isolobal borane-fragment–metal-fragment substitution, then the reaction products of I and II with $Fe_2(CO)_9$ are conveniently explained. Note that metallaborane cluster expansion by metal-fragment addition, partially driven by H_2 elimination, has already been demonstrated.[19] Hence, we postulate the formal reaction path

$$[B_2H_{6-n}Fe_2(CO)_6]^{n-} + Fe_2(CO)_9 \rightarrow [B_2H_{4-n}Fe_3(CO)_{10}]^{n-} + H_2$$

$$[B_2H_{4-n}Fe_3(CO)_{10}]^{n-} \rightarrow [BH_{3-n}Fe_3(CO)_{10}]^{n-} + (1/m)(BH)_m$$

$$[B_2H_{4-n}Fe_3(CO)_{10}]^{n-} + [Fe(CO)_3] \rightarrow [HFe_4(CO)_{12}BH_{2-n}]^{n-} + (1/m)(BH)_m$$

$$n = 0, 1$$

Even though other pathways are possible, this mechanism provides a stoichiometric basis for understanding the results. Specifically, we suggest that addition of a metal fragment to the four-atom cluster, in a manner analogous to that previously established[19] for $[HFe_3(CO)_9BH_3]^-$, results in an intermediate with the Fe_3B_2 core. Under the reaction conditions, we suggest that this intermediate can either lose a BH fragment or undergo replacement of a BH fragment with a metal fragment.[21] The former leads to $[BH_{3-n}Fe_3(CO)_9]^{n-}$, while the latter leads to the "butterfly" cluster $[HFe_4(CO)_{12}BH_{2-n}]^{n-}$. This mechanism limits the maximum yield of boron in the products to 50% of that contained in the reactants. For the reaction of anion II with $Fe_2(CO)_9$, approximately 35% (by NMR spectroscopy, Figure 6) of the initial boron is observed in the two ferraborane products. The form of the lost boron is not known, but it may be "polymeric" BH.[22]

Electronic Structure and Energetics. The electronic structure of I has been discussed previously on the basis of hydrogen arrangement Ib.[23] As we have demonstrated above, this structure is at best an intermediate in the hydrogen-exchange mechanism. Hence, the essential differences in electronic structure resulting from changes in endo-hydrogen location have been investigated by using the Fenske–Hall technique.

The most significant conclusion to be derived from the calculations (supplementary material) is the absence of large differences between the structures examined. In fact, even structures that

(18) Rudolph, R. W.; Parry, R. W. *Inorg. Chem.* **1967**, *6*, 1068. Onak, T.; Leach, J. B.; Anderson, S.; Frisch, M. J. *J. Magn. Reson.* **1976**, *23*, 237.
(19) Housecroft, C. E.; Fehlner, T. P. *Organometallics* **1986**, *5*, 379.
(20) Vahrenkamp, H. *Adv. Organomet. Chem.* **1986**, *22*, 169.
(21) In transition metal cluster systems, substitution of a metal vertex by the incoming metal fragment has been observed: Kolis, J. W.; Holt, E. M.; Hriljac, J. A.; Shriver, D. F. *Organometallics* **1984**, *3*, 496. On the other hand, in borane cage systems loss of BH vertices to undefined products is observed: Onak, T. In *Boron Hydride Chemistry*; Muetterties, E. L., Ed.; Academic: New York, 1975; p 349. The loss of a BH vertex in the formation of metallaboranes has also been observed: Grimes, R. N. *Acc. Chem. Res.* **1983**, *16*, 22.
(22) Holtzmann, R. T., Ed. *Production of the Boranes and Related Research*; Academic: New York, 1967.
(23) Andersen, E. L.; DeKock, R. L.; Fehlner, T. P. *Inorg. Chem.* **1981**, *20*, 3291.

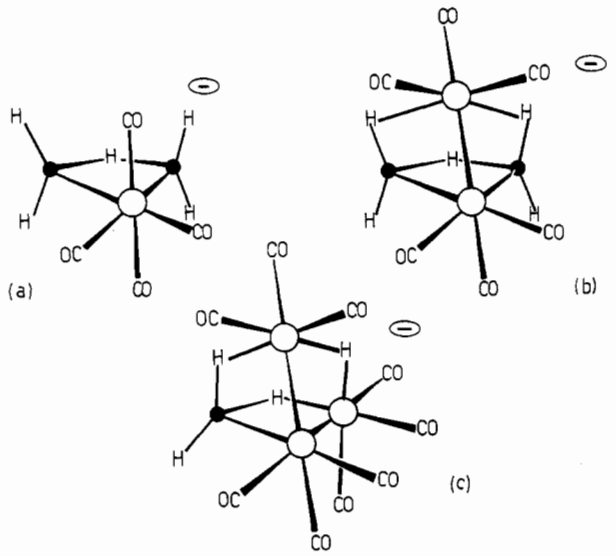

Figure 7. Schematic comparison of the geometric structures of (a) $[B_2H_5Fe(CO)_4]^-$, (b) $[B_2H_5Fe_2(CO)_6]^-$, and (c) $[BH_4Fe_3(CO)_9]^-$.

appear unlikely are not eliminated by the calculations. Indeed, some face-bridged structures are predicted to be slightly more stable than the edge-bridged ones! The similar energies of the edge-bridged and face-bridged structures are consistent with the fluxional behavior described above in that any real intramolecular mechanism for the hydrogen-exchange processes must involve hydrogen movement across faces to an available edge. We conclude that the factors determining the relative stabilities of different endo-hydrogen distributions are indeed subtle.

Comparison of II with $[B_2H_5Fe(CO)_4]^-$. Shore et al. have prepared and characterized the ferraborane $[B_2H_5Fe(CO)_4]^-$, consisting of a diborane ligand coordinated to a monoiron carbonyl fragment.[24] Hence, we can now compare the structural properties of a $B_2H_5^-$ moiety when bound to one vs two metal atoms. As is seen in Figure 7, II (structure II(trans)) can be formally generated from $[B_2H_5Fe(CO)_4]^-$ by replacing an axial CO ligand with the two-electron donor $Fe(CO)_3$. Two of the former BH(terminal) hydrogens of the B_2H_5 moiety satisfy the empty orbitals on the newly added $Fe(CO)_3$ fragment. Although II is fluxional in that the FeHB and BH(terminal) protons exchange rapidly at room temperature, in neither the mono- or diiron compound do the terminal (or FeHB) protons exchange with the BHB proton on the NMR time scale.

Comparison of II with $[BH_4Fe_3(CO)_9]^-$. Anion II can also be structurally compared with $[BH_4Fe_3(CO)_9]^-$ by using the isolobal relationship between BH and $Fe(CO)_3$ fragments (Figure 7b vs Figure 7c).[5] Note that the static-hydrogen positions, after replacement of the main-group fragment by the isolobal transition-metal fragment, are the same. This also holds true for a comparison of the neutral triiron ferraborane $HFe_3(CO)_9BH_4$ and I. If endo hydrogens behave as protons on a cluster surface, seeking out the maximum available electron density, then the Fe_2B_2 and Fe_3B clusters may have similar cluster charge distributions; i.e., BH is an excellent mimic for $Fe(CO)_3$. Although $HFe_3(CO)_9BH_4$ exhibits an endo-hydrogen distribution analogous to that of I, the fluxional processes exhibited by the two compounds are different.

Experimental Section

All manipulations were carried out in a high-vacuum line or under an atmosphere of nitrogen with standard Schlenk techniques.[25] $Fe(CO)_5$ (Alfa) was distilled under reduced pressure. $LiBH(C_2H_5)_3$ (1 M in THF) and BH_3·THF (1 M in THF containing <0.05 M $NaBH_4$ as stabilizer) were obtained from Aldrich Chemical Co. and used as received. Ph_4AsCl was obtained from Aldrich. $N(C_2H_5)_3$ (Eastman) was distilled before use. H_3PO_4 (85%), CH_3OH, and CH_2Cl_2 were saturated with N_2 gas before use. Hexanes and $(C_2H_5)_2O$ were distilled under nitrogen before use.

^1H (300-MHz) and ^{11}B (96.3-MHz) NMR spectra were recorded on a Nicolet NB 300 spectrometer. ^1H (100-MHz) NMR spectra were recorded on a Varian XL100 spectrometer. Infrared spectra were recorded on a Perkin-Elmer 983 spectrometer, and mass spectra, on an AEI MS-902 mass spectrometer.

The Mössbauer spectra were obtained at 78 K on a conventional constant-acceleration spectrometer that utilized a room-temperature rhodium-matrix cobalt-57 source and was calibrated at room temperature with natural-abundance α-iron foil. The spectra were fit to symmetric quadrupole doublets with Lorentzian line shapes by using standard least-squares computer minimization techniques.

Preparation of $B_2H_6Fe_2(CO)_6$. $Fe(CO)_5$ (0.675 mL; 5 mmol), $LiBHEt_3$ (5 mL; 5 mmol), and BH_3·THF (10 mL; 10 mmol) were combined at −78 °C in a 50-mL round-bottom flask containing a magnetic stirring bar. The flask was placed in an ice–water bath and the mixture stirred for 3 h, during which time the solution changed from yellow to deep red-brown. The solvent was then removed under reduced pressure. Hexanes (25 mL) and H_3PO_4 (15 mL) were added to the solid residue, and the mixture was stirred vigorously for 30 min. The hexane layer turned brown, leaving only a small amount of solid material undissolved. The solvent was removed from the hexane layer under reduced pressure at 0 °C. The resulting brown residue was pumped into a −196 °C trap for 6 h, after which its contents were fractionated through 0, −15, −45, and −196 °C traps. A yellow-brown air-sensitive liquid condensed in the −15 °C trap and was shown to be I, as described above. NMR yield based on boron was 10%. MS for $^{56}Fe_2{}^{11}B_2{}^{12}C_6{}^{16}O_6{}^1H_6^+$: 307.9048 calcd, 307.9066 exptl. IR (hexane), cm^{-1}: ν_{BH} 2530 (w); ν_{CO} 2091 (s), 2046 (vs), 2026 (s), 2022 (s), 1996 (s), 1990 (s).

$[B_2H_5Fe_2(CO)_6]Ph_4As$. Hexanes (5 mL) were frozen at −196 °C onto a sample of $B_2H_6Fe_2(CO)_6$. The mixture was warmed to 20 °C to dissolve the ferraborane, yielding a yellow solution. A solution of Ph_4AsCl in CH_3OH (0.1 g in 3 mL) was added under N_2 and the mixture stirred for 5 min, during which time the CH_3OH layer turned orange. The mixture was pumped dry for several hours, and $(C_2H_5)_2O$ (10 mL) was condensed onto the residue. The resulting orange solution was filtered and the solvent removed from the filtrate, leaving an orange solid. The yield was quantitative as measured by ^{11}B NMR spectroscopy. IR (toluene), cm^{-1}: ν_{BH} 2470 (w); νCO 2022 (m), 1965 (s), 1935 (sh), 1928 (m). All attempts at growing crystals resulted in decomposition and the formation of crystals of $[HFe_3(CO)_{11}]Ph_4As$.

$[B_2H_5Fe_2(CO)_6](C_2H_5)_3NH$. To a hexane solution of $B_2H_6Fe_2(CO)_6$ were added a few drops of $(C_2H_5)_3N$. An orange precipitate formed immediately, and the mixture was pumped dry for several hours. Extraction in $(C_2H_5)_2O$ followed by removal of the solvent from the filtered extract yielded an orange solid, the solution NMR spectroscopic properties of which were similar to those of the Ph_4As^+ salt.

Protonation/Deprotonation. A sample of $B_2H_6Fe_2(CO)_6$ dissolved in hexanes was placed into a 10-mm NMR tube containing an external standard of n-$Bu_4NB_3H_8$. The ^{11}B NMR spectrum was recorded, and the relative areas of each resonance were measured. $N(C_2H_5)_3$ (2 drops) was added to the tube and the mixture shaken for 5 min. The hexanes were removed under reduced pressure, and the resulting solid was dissolved in CH_3OH. The ^{11}B spectrum of the CH_3OH solution was similarly recorded, and the observed anion resonance was 95% of the neutral signal intensity. The CH_3OH was then removed under vacuum, and hexanes (3 mL) and H_3PO_4 (1 mL) were added. After 15 min of stirring, the yellow hexane layer was removed and its ^{11}B NMR spectrum recorded. The observed neutral ferraborane resonance was 95% as intense as that of the original anion.

Reactivity of I and II with $Fe_2(CO)_9$. The ^{11}B NMR signals of 0.2 mmol of $B_2H_6Fe_2(CO)_6$ in 5 mL of hexane and 0.15 mmol of $[B_2H_5Fe_2(CO)_6]PPN$ in 5 mL of CH_2Cl_2 were calibrated against an external standard of $[B_3H_8]N(C_4H_9)_4$ in $(CD_3)_2CO$. The ferraborane solutions (at 25 °C) were then transferred to 25-mL round-bottom flasks containing a large excess of $Fe_2(CO)_9$. Periodically, the solution phase was transferred back into the NMR tube with the standard and the ^{11}B spectrum recorded. The integral of the ^{11}B signal relative to the standard was taken to be a measure of the concentration of the ferraborane.

Calculations. Fenske–Hall calculations[26] were carried out on I and II with the structures listed in Table V (see Chart I). The geometries of the clusters were constructed by using reasonable structural parameters

(24) Medford, G.; Shore, S. G. *J. Am. Chem. Soc.* **1978**, *100*, 3953. DeKock, R. L.; Deshmukh, P.; Fehlner, T. P.; Housecroft, C. E.; Plotkin, J. S.; Shore, S. G. *J. Am. Chem. Soc.* **1983**, *105*, 815.

(25) Shriver, D. F. *Manipulation of Air Sensitive Compounds*: McGraw-Hill: New York, 1975; p 241.

(26) Hall, M. B.; Fenske, R. F. *Inorg. Chem.* **1972**, *11*, 768. Hall, M. B. Ph.D. Thesis, University of Wisconsin, Madison, WI, 1971. Fenske, R. F. *Pure Appl. Chem.* **1971**, *27*, 61.

derived from the known structures of closely related compounds.[4,5] The structure of Ib, which has been discussed extensively in the earlier calculational work,[23] was used as the "standard" geometry. That is, all hydrogen arrangements investigated were examined with this fixed cluster core geometry. However, as the Fe-B distance in this model was 2.21 Å, several calculations were carried out with the non-hydrogen-bridged Fe-B edges set at 2.00 Å. As there were no large differences in the results and as the shorter Fe-B distances distorted the cluster, not all structures were investigated in this fashion. The basis functions and exponents used in the calculations were the same as used previously.[23]

Acknowledgment. The support of the National Science Foundation under Grant CHE 84-08251 is gratefully acknowledged. We also thank the Notre Dame Computing Center for computing time and the donors of the Petroleum Research Fund, administered by the American Chemical Society, for support of this research.

Registry No. Ia, 67517-57-1; II·Ph_4As, 110796-05-9; II·$(C_2H_5)_3NH$, 110796-07-1; II·PPN, 110796-08-2; III, 80572-82-3; IV, 108008-76-0; $[BH_2Fe_3(CO)_{10}]^-$, 92078-18-7; $Fe(CO)_5$, 13463-40-6; $Fe_2(CO)_9$, 15321-51-4.

Supplementary Material Available: Text, one table, and one figure summarizing pertinent results of Fenske-Hall calculations (3 pages). Ordering information is given on any current masthead page.

Contribution from the Department of Chemistry and Laboratory for Molecular Structure and Bonding, Texas A&M University, College Station, Texas 77843

Further Study of Metal-Metal Bond Lengths in Homologous Edge-Sharing Bioctahedral Complexes

Jo Ann M. Canich, F. Albert Cotton,* Lee M. Daniels, and Diane B. Lewis

Received May 19, 1987

Four new compounds have been prepared and characterized structurally: $Mo_2Cl_6(dmpm)_2$ (**1**), $W_2Cl_6(dmpm)_2$ (**2**), $W_2Cl_6(dppm)_2$ (**3**), and $Re_2Cl_6(dmpm)_2$ (**4**) (where dmpm = $Me_2PCH_2PMe_2$ and dppm = $Ph_2PCH_2PPh_2$). The structural data for these four compounds combined with similar data previously published[1] for five other homologous compounds provide a more detailed and secure picture of how M-M bonding in edge-sharing bioctahedral complexes depends on the number of d electrons available. The previous conclusion that in molecules of the type studied here, i.e., $M_2Cl_6(dRpm)_2$, the M-M bonding orbitals are filled in the order σ, π, δ^*, δ, π^*, σ^* is validated. However, the row (second or third transition series) from which the metal atom originates and the choice of diphosphine ligand (dmpm or dppm) are found to be factors of greater importance than was previously recognized. Crystallographic data for the new compounds as well as their M-M distances are as follows: **1**, $P2_1/n$ with a = 6.976 (2) Å, b = 15.559 (6) Å, c = 11.000 (6) Å, β = 94.24 (3)°, and Z = 2, Mo-Mo = 2.7394 (5) Å; **2**, $P2_1/c$ with a = 8.625 (2) Å, b = 20.229 (3) Å, c = 8.676 (2) Å, β = 92.80 (2)°, and Z = 2, W-W = 2.6663 (4) Å; **3**, $C2/c$ with a = 23.025 (9) Å, b = 10.938 (4) Å, c = 21.722 (9) Å, β = 117.61 (3)°, and Z = 4, W-W = 2.691 (1) Å; **4**, $P2_1/n$ with a = 6.9140 (6) Å, b = 15.358 (1) Å, c = 10.8621 (9) Å, β = 94.894 (7)°, and Z = 2, Re-Re = 2.5807 (4) Å.

Introduction

Several years ago we reported structural results[1] on a series of compounds of type I, from which certain conclusions were drawn as to the ordering of the σ, π, δ, δ^*, π^*, and σ^* orbitals that are primarily involved in the M-M interaction. It was stressed in

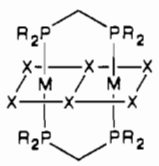

I: R = CH_3, C_6H_5; X = Cl

the discussion of that work that if M to M distances in edge-sharing bioctahedral complexes[2] are to be used as an index of the strength of the M-M bonding it is important to maintain all factors other than the number of electrons available to fill such orbitals as nearly invariant as possible. Such factors as the oxidation state of the metal, the size of the metal atoms, and the identity of the ligands are crucial. In the series of five compounds presented in that earlier study we were forced to compromise slightly on this requirement. In particular, we included complexes formed by both second- and third-transition-series elements and used both $(CH_3)_2PCH_2P(CH_3)_2$ (dmpm) and $(C_6H_5)_2PCH_2P(C_6H_5)_2$ (dppm) ligands because of our inability to synthesize a series of compounds confined entirely to one transition series and to one of the two diphosphine ligands. We suggested that, because of the well-known effect of the lanthanide contraction, the employment of both second- and third-row metal atoms would not have a serious effect and supported this with data for analogous Nb and Ta complexes where the M-M distances differed only slightly compared to the differences from one bond order to another. As for the changes from dmpm to dppm, we had no control experiment but assumed that this would also be only a tolerably minor perturbation.

We have now been able to prepare and structurally characterize four more compounds of type I. These provide direct tests of both of the previous assumptions. They show (a) that the assumptions were less satisfactory than we had believed but (b) that the main conclusion as to the ordering of the molecular orbitals is still valid. The four new compounds and their identifying numbers that will be used throughout are $Mo_2Cl_6(dmpm)_2$ (**1**), $W_2Cl_6(dmpm)_2$ (**2**), $W_2Cl_6(dppm)_2$ (**3**), and $Re_2Cl_6(dmpm)_2$ (**4**).

Experimental Section

All manipulations were carried out under an atmosphere of argon by using standard Schlenk and vacuum line techniques. Commercial-grade solvents were purchased from Fischer Scientific Co. Toluene and hexane were distilled from benzophenone ketyl prior to use, while CH_2Cl_2 was dried by distillation from phosphorus pentoxide. Bis(dimethylphosphino)methane (dppm) was purchased from Organometallics, Inc., and chlorine gas was obtained from Matheson Gas Products, Inc. The infrared and visible spectra were recorded on Perkin-Elmer 783 and Cary 17D spectrophotometers, respectively.

Preparation of Crystalline Compounds. Compound 1. The starting material, $Mo_2Cl_4(dmpm)_2$, was prepared by a literature method.[3] A 0.25-g amount of $Mo_2Cl_4(dmpm)_2$ dissolved in 25 mL of CH_2Cl_2 was placed in a test tube, which was then fitted with a septum. Chlorine gas was introduced through the septum via a disposable pipet for 45-90 s. During this time the solution changed from blue to bright orange, and the solvent was immediately removed under vacuum. The product was recrystallized by slow evaporation of a CH_2Cl_2 solution (yield 83%).

Compound 2. The starting material, $W_2Cl_4[P(n\text{-}Bu)_3]_4$, was prepared by a literature method.[4] To a 100-mL round-bottom flask equipped with

(1) Chakravarty, A. R.; Cotton, F. A.; Diebold, M. P.; Lewis, D. B.; Roth, W. J. *J. Am. Chem. Soc.* **1986**, *108*, 971.
(2) Cotton, F. A. *Polyhedron* **1987**, *6*, 667.
(3) Cotton, F. A.; Falvello, L. R.; Harwood, W. S.; Powell, G. L.; Walton, R. A. *Inorg. Chem.* **1986**, *25*, 3949.

0020-1669/87/1326-4046$01.50/0